Proceedings of ITC18, 2008

Hydrogen Concentration and Crystal Structure of Carbon Film Produced at the Duct of Local Island Divertor in Large Helical Device

Tomoya Hirata[1)], Yuji Nobuta[1)], Tomoaki Hino[1)], Suguru Masuzaki[2)], Naoko Ashikawa[2)], Yuji Yamauchi[1)], , Yuko Hirohata[1)], Akio Sagara[2)], Kiyohiko Nishimura[2)], Nobuyoshi Ohyabu[2)], Nobuaki Noda[2)], Akio Komori[2)], Osamu Motojima[2),] LHD Experimental Group[2)]

1) Laboratory of Plasma Physics and Engineering, Hokkaido University, Sapporo, 060-8628, Japan

2) National Institute of Fusion Science, Toki-shi, Gifu-ken, 509-5292, Japan

Two sets of material probes were installed at the pumping duct of the Local Island Divertor (LID) in the Large Helical Device (LHD) during 9th (2005) and 10th (2006) experimental campaign. One set of the material probes were faced to the LID head which consists of carbon fiber composite (CFC) tiles, and the other set were far from the head. After the campaigns, the material probes were extracted, and their surface morphology, the depth profile of atomic composition, thickness of the deposition layer on them, the amount of retained hydrogen in the layer and crystal structure of the layer were investigated. The value of hydrogen concentration in the carbon layers on the probes faced to the LID head was H/C = 0.55 in the atomic ratio. On the other hand, the value on the probes far from the head was significantly large, H/C = 1.25 in the atomic ratio. The microstructure analysis of the carbon deposition layers using Raman spectroscopy indicates that the layers were polymer like amorphous hydrogenated carbons, which was possibly resulted from the large deposition of chemically sputtered hydrocarbon on the probes. As the result, the co-deposited layers with a large amount of hydrogen were formed.

Keywords: Carbon deposition layer, Co-deposition, Hydrogen retention, Local Island Divertor, Large Helical Device,

1. Introduction

One of the important issues for ITER is to evaluate in-vessel tritium inventory because the retained amount of tritium in ITER is limited below 350 g. Carbon fiber composite (CFC) will be used for a divertor plate material of ITER. Carbon materials are easily eroded by incident hydrogen isotopes ions for physical and chemical sputtering, and carbon co-deposits with plenty of hydrogen isotopes in the vicinity of the divertor. When tritium is employed for fuel gas in ITER, large amount of tritium will be retained in the deposited carbon layer. So the characterizations of the carbon co-deposition layer and its hydrogen isotope retention are important concerns associated with the reactor safety [1].

In tokamak devices, hydrogen retention behaviors in carbon components, such as divertor tiles, have been investigated so far [2-4]. It was found that the tritium retention in the shadow area could be significantly large. The CFC was also employed for divertor material of the local island divertor (LID) in the Large Helical Device (LHD).

The CFC tiles were eroded by hydrogen ion bombardment and carbon co-deposits with hydrogen in the pumping duct of LID, which is shadowed from the plasma.

In this paper, we focused on the co-deposited carbon layer produced in the pumping duct of LID in 9th (2005) and 10th (2006) experimental campaign. The relationship between the structure of carbon layer, wall temperature and hydrogen concentration was investigated.

2. Experimental

In LHD, the LID experiments have been conducted since 2003, in addition to intrinsic helical divertor experiments [5]. Figure 1 shows a schematic view of the LID configuration. A divertor head that is covered by the neutralizer plates made of CFC is inserted into the m/n=1/1 magnetic island in the horizontally elongated cross-section where the width of the island is maximum (about 20 cm). The pumping duct surrounds the divertor head, and it works as a baffle. Outer separatrix of the island connects the divertor head as the divertor legs, and the last closed flux surface is determined by the inner separatrix of the island. Plasma-surface interaction occurs only at the divertor head ideally, and thus the wet area (< 0.1 m^2) is less than one tenth of that of helical divertor. Therefore, the divertor head receives much higher heat and particle fluxes than those to the helical divertor plates, and a considerable amount of carbon was eroded and co-deposited with hydrogen during the experiments [6]. The crystal structure and the hydrogen retention properties of the co-deposited carbon layers in the vicinity of LID head were investigated with a technique of material probe [7]. During each 9th (2005) and 10th (2006) experimental campaign, silicon and stainless steel (SUS316L) probes were installed at four

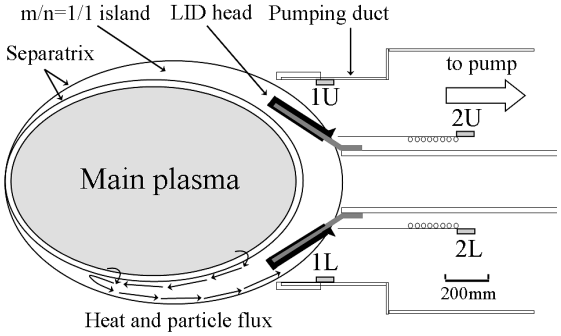

Fig.1 Schematic view of the LID configuration. The LID head is inserted into the m/n=1/1 magnetic island. The black parts on the LID head are made of carbon (graphite or CFC), and the gray parts are the base structure of the head that is made of SUS316. Material probes (1U, 1L, 2U, 2L) were installed inside the pumping duct. The neutral gas pressure in the pumping duct close to the LID head was considered to be ~1 Pa.

author's e-mail: y-nobuta@eng.hokudai.ac.jp

positions in the pumping duct as shown in Fig.1. Two probe sets (1U, 1L) were placed inside the pumping duct, which was faced to the LID head and have 200 mm distance from the tip of the pumping duct. The other sets of probes (2U, 2L) were 870 mm far from the tip of the pumping duct and had shallow line of sight to the head. In these experimental campaigns, hydrogen gas was employed for the LID discharges. The numbers of the discharge with the LID configuration were 707 (9th) and 313 (10th).

The stainless steel probes were used for analysis of surface morphology and gas retention, and silicon probes were used to investigate depth profile of atomic composition, the thickness and the crystal structure of the deposited carbon layers, respectively. The size of each probe is 10 mm × 20 mm × 1 mm. Typical surface temperatures of the head near the strike point and the pumping duct near the LID head estimated from thermocouple measurements were approximately 1000 K and 600 K, respectively. At the probe position close to the head (1U, 1L), the maximum wall temperature during the discharge was ~570 K. In the case of the other probe position far from the head (2U, 2L), the wall temperature during discharge was in the range from RT to 323 K.

After each experimental campaign, the probes were extracted and analyzed using scanning electron microscope (SEM), Auger electron spectroscopy (AES), surface roughness meter, thermal desorption spectroscopy (TDS), X-ray deflection, and Raman spectroscopy.

3. Results and discussion

3.1 Surface morphology

Figures 2 (a) and (b) show the SEM photographs of the 1U and 2U surfaces after the 9th experimental campaign. On the surface of 1U, sub-micron size protuberant structures were observed. On the other hand, the surface of 2U was smooth compared to 1U. The surfaces conditions of 1L and 2L were similar to those of 1U and 2U, respectively. This difference of surface morphologies between 1U and 2U might be caused by the deposition process of sputtered carbon atoms. The neutral gas pressure in the pumping duct close to the LID head reached up to ~1 Pa. Therefore, sputtered carbon particles were scattered before they redeposit on the probes. And then, they incident to the surface of the probe close to the head from random angle and deposit selectively on the protuberant structure. This is one of the possible explanation for the formation of protuberant structure. On the other hand, the smooth surface might result from the direct deposition of chemically sputtered hydrocarbon.

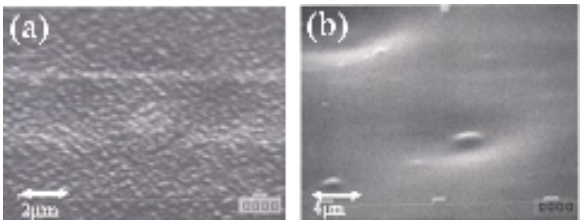

Fig.2 SEM images of the surface morphologies of the stainless steel probes, (a) 1U and (b) 2U after 9th experimental campaign.

3.2 Atomic composition and film thickness of deposited layer

In AES analysis, Ar ion with an energy of 3keV was used for sputtering. The depth of the crater formed by the Ar ions bombardment was measured by a surface roughness meter, and then the depth was estimated from the sputter-etching time. The concentration of oxygen was below 1 at.%, which were similar to those of other probes. Figure 3 shows the thickness of the deposition layer measured by using the surface roughness meter. The thickness of the layers on 1L and 1U after 9th experimental campaign was in the range from 500 to 700 nm. On the other hand, the thickness on 2L and 2U was in the range from 160 to 200 nm. In 10th experimental campaign, the thickness was approximately a half of that in 9th experimental campaign. This is owing to the reduced number of hydrogen discharge in 10th experimental campaign. Assuming the typical duration time in a LID discharge to be 2 s, the deposition rates of the carbon on 1U and 2U are estimated to be 0.64 nm/s and 0.14 nm/s, respectively

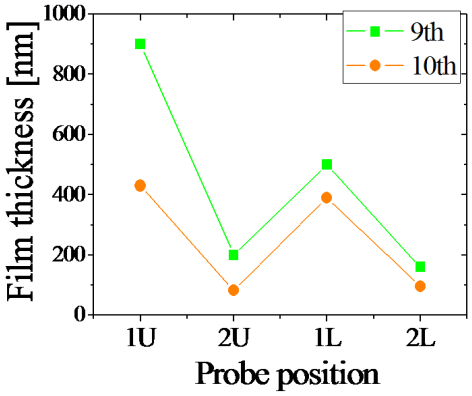

Fig.3 The thickness of the deposition layer on the probes.

3.3 Hydrogen retention

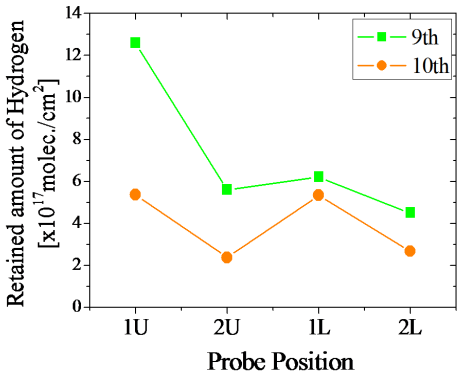

Fig.4 Retained amounts of hydrogen of the deposited carbon films on the probes.

Figure 4 shows the retained amounts of hydrogen in the probes. Most of retained hydrogen desorbed in form of hydrogen molecular during the TDS measurements. In the case of 10th experimental campaign, the retained amount of hydrogen was approximately a half of that in 9th experimental campaign. These results indicate that the retained amount of hydrogen of each position was roughly proportional to the deposited carbon film thickness.

3.4 Crystal Structure of Carbon Films

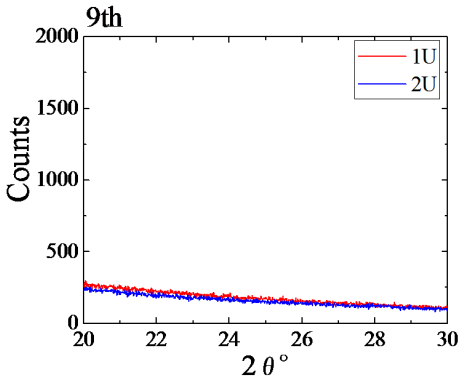

Fig.5 X-ray diffraction patterns of the deposited carbon films after 9th experimental campaign.

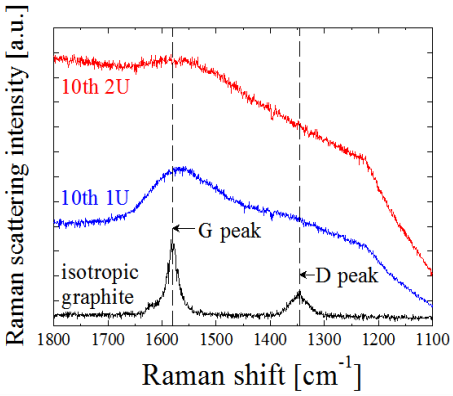

Fig.6 Raman spectra of the surface of the carbon film on the probes after 10th experimental campaign.

Figure 5 shows X-ray diffraction patterns of the carbon deposition layers after 9th experimental campaign. In the case of graphite, (002) X-ray deflection peak appears around 2θ =26 degree. In the case of the probes, however, no peak was observed. This result indicates that the structures of the carbon layers on 1U and 2U probes were amorphous. Figure 6 shows Raman spectra of the carbon layers on the probes in 10th experimental campaign. Raman spectrum of isotropic graphite has two peaks as shown in the figure with the black line. The peak at 1580 cm^{-1} is called "G" peak which originates from graphite structure. The other peak at 1355 cm^{-1} is called "D" peak which originates from defects [16]. The spectra of the carbon films on the probes were not similar to that of isotropic graphite but were similar to that of polymer-like amorphous hydrogenated carbon film [16]. The spectra of 1U have a broad peak around 1580 cm^{-1}, indicating that this layer contained carbon hexagonal structure like graphite. On the other hand, the "G" peak was not clear in the spectra of 2U. The carbon layer of 2U is considered to be more polymerized than 1U, which might have been caused by deposition of chemically sputtered hydrocarbon at low temperature.

3.5 Hydrogen concentration

In the present study, the mass densities of the carbon layers on the probes were not measured directly. For the estimation of hydrogen concentration, it is necessary to evaluate the density of carbon layers produced in the LID experiments. For this purpose, we prepared amorphous hydrogenated carbon film (a-C:H film) by using a magnetron sputtering device. The discharge gases in this device were argon and hydrogen gas with the mixture ratio of 1/20 in H_2/Ar. Input power was 1 kW. The distance between substrate and graphite target was 3.5 cm. The discharge pressure was kept at 1.5 Pa. The discharge time was 2 hours. The film thickness of the produced a-C:H film was estimated to be 160 nm by using the surface roughness meter. The mass density of the a-C:H film was estimated to be 0.98 g/cm^3 by a weight gain measurement. Next, we measured the etching rate of the a-C:H film by Ar ion etching in the AES apparatus to compare the rate to that of the LID samples. For the etching rate is proportional to the mass density, we can estimate the mass densities of the LID samples. The density of carbon film on the probes close the LID head (1U, 1L) was estimated to be 0.93 g/cm^3 and that of the probes far from the head (2U, 2L) was estimated to be 0.90 g/cm^3. These values were lower than that of isotropic graphite (1.8 g/cm^3), and thus, they are so called "soft" deposition layer. Using the volume of the deposition layer, which was calculated using the surface area and the thickness of the layer, and the estimated mass density, a number of carbon atoms in the carbon layer was obtained. Using the number and the measured amount of the retained hydrogen with the TDS measurement, the hydrogen concentration (H/C) was obtained for each sample. The atomic ratios of H/C for 1U, 1L, 2U and 2L were estimated to be 0.53, 0.55, 1.26 and 1.24 after 9th experimental campaign, and H/C = 0.52, 0.58, 1.25 and 1.27 after 10th experimental campaign. Fig.7 shows the relationship between the atomic ratio of H/C for the probes and the maximum temperature of the probes during the LID discharge. The deuterium concentrations in graphite after the irradiation of deuterium ion beam with the energy of 1.0 keV at different graphite temperature [11,13] are also plotted in Fig.7. In the laboratory experiment, the deuterium concentration in graphite, D/C, after deuterium ion irradiation at the temperature from room temperature

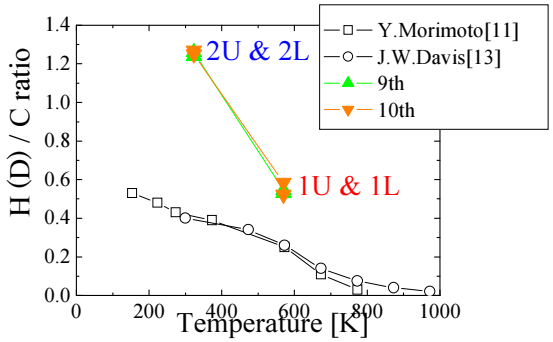

Fig.7 The relationship between the hydrogen concentrations of carbon films produced in the location of probes and the temperature on the surface of probes. In addition, the data of the deuterium concentration in graphite after deuterium ion irradiation with the energy of 1.0 keV at temperature from 153 K to 773 K is also shown. [11, 13]

to 570 K is approximately D/C=0.3 [11, 12, 13]. The H/C ratios on 1U and 1L probes were double of this value. For the carbon layer on 2U and 2L probes, the hydrogen concentrations were approximately triple of the graphite case. The large hydrogen concentration in 2U and 2L probes was associated with for polymerized amorphous structure in the carbon layers deposited on 2U & 2L probes. This result suggests that the characteristics of the carbon layers produced in the pumping duct of the LID were dominated by the deposition of hydrocarbon. In JT-60U, the atomic ratio of D/C for a carbon film deposited on the divertor tile was < 0.04 with the divertor temperature above 600 K [14]. Compared with this value, the atomic ratio of H/C in the carbon film produced in the vicinity of LID head was much higher. On the other hand, the D/C ratio for the carbon film deposited on the divertor tiles in JET MK-IIA divertor with the temperature below 500 K [14] was 0.1~0.4, and the D/C ratio in the re-deposited layers on the louvers, which was shadowed from the plasma and was kept at low temperature, was 0.8 [2,15]. This value was close to that of the co-deposited carbon film produced in the vicinity of LID obtained in the present study. The present results indicates that the hydrogen concentration of co-deposited layer could be large compared to that at the plasma-wetted region.

4. Conclusion

The relationship between the structure of carbon layer and hydrogen concentration in the layer on material probes in the vicinity of LID in LHD was investigated. The hydrogen concentration in the carbon films (H/C) on the probes close to the LID head (1U and 1L) where wall temperature was 570 K was around 0.55. On the othedddr hand, H/C in the carbon films on the probes far from the head (2U and 2L) where wall temperature 327 K was significantly large, 1.25. These values were several times larger than those in graphite after deuterium ion beam irradiation. The structures of these carbon films were polymer like amorphous hydrogenated carbon. This suggests that the hydrogen concentration in co-deposited carbon layer formed could be large due to deposition of hydrocarbon.

Acknowledgements

This work was supported by the Collaboration Research Program for Large Helical Device (NIFS04KOBS005, KLPP301) in National Institute for Fusion Science, and partly supported by the JSPS-CAS Core University Program in the field of Plasma and Nuclear Fusion.

Reference

[1] G. Federici et al, Nucl. Fusion **41**, 1967 (2001).
[2] J. P. Coad et al, J. Nucl. Mater. **290-293**, 224 (2001).
[3] M. Mayer et al, J. Nucl. Mater. **290-293**, 381 (2001).
[4] K. Masaki et al, J. Nucl. Mater. **337-339**, 553 (2005).
[5] T. Morisaki et al, J. Nucl. Mater. **337-339**, 154 (2005).
[6] S. Masuzaki et al, J. Nucl. Mater **363-365**, 314 (2007)
[7] T. Hino et al, Nucl. Fusion **44**, 496 (2004).
[8] Y. Yamaichi et al, Vacuum. **47**, 6-8, 973 (1996)
[9] J. Winter et al, Nucl. Instr. And Meth. In Phys. Res. **B23**, 538(1987).
[10] Y. Ishimoto et al, J. Nucl. Mater. **350**, 301 (2006)
[11] Y. Morimoto et al, J. Nucl. Mater. **313-316**, 595 (2003).
[12] J. Roth et al, J. Nucl. Mater. **93-94**, 601 (1980).
[13] J. W. Davis et al, J. Nucl. Mater. **217**, 206 (1994).
[14] T. Tanabe, Fusion Eng. Des. **81**, 139 (2006)
[15] Y. Hirohata et al, J. Nucl. Mater. **363-365**, 854 (2007)
[16] Paul K. Chu et al, Mater Chem and Phys. 96 (2006) 253-277